



# Heat input control in horizontal lap joint welding through active wire preheating in GMAW-P

Fernando Matos Scotti<sup>1,2</sup> · Maximilian Pudenz<sup>1,2</sup> · Sarah Perrin<sup>1,3</sup> · Erwan Siewert<sup>1</sup> · Jean Pierre Bergmann<sup>2</sup>

Received: 26 September 2023 / Accepted: 30 November 2023 / Published online: 19 December 2023  
© International Institute of Welding 2023

## Abstract

In gas metal arc welding (GMAW) the arc power, in general, increases when the wire feed speed is increased. Thus, controlling heat input into the workpiece becomes a challenge, especially when trying to increase productivity. Metal transfer modes such as pulsed and controlled short circuit have been successfully applied to allow smooth metal transfer with relatively low energy. The effect of increasing the electrified length of the electrode or decreasing wire diameter in reducing current has been known for years. However, to some extent, this effect is limited to the physical conditions when using a large distance from contact tip to workpiece. To further increase melting efficiency and reduce arc power the torch presented in this paper includes a second electric circuit into GMAW to preheat the wire by ohmic heating before it reaches the main circuit. In this context, the objective of this work was to verify the effects of active wire preheating in GMAW in lap joint case in terms of electric signal behavior, thermal behavior in the plate, and weld bead formation. By increasing the preheating current, significant reduction in arc power was achieved. This reflects on the resulting weld by avoiding molten pool sagging, reducing fused area, silicate formation, and backside oxidation. The reduction in heat input resulted finally in a smaller heat affected zone which had a finer microstructure. In conclusion, the use of active wire preheating in GMAW expands the potential for increasing productivity and controlling heat input into the workpiece.

**Keywords** Heat input · GMAW · Lap joints · Ohmic heating · Out of position

## 1 Introduction

For multiple industry segments where metal joining is required, improving the productivity and reliability of welding process is a constant challenge. Within the arc welding processes, gas metal arc welding (GMAW) is known for reaching high deposition rates while being relatively easy to use in its semi-automated or fully automated applications.

Within this process, many improvements and derivative processes were developed by researchers and specialized companies aiming at high deposition rates, improved metal transfer (low spatter generation), and controlled heat input. Such innovations are usually based on advanced electronic control of the power source, double wire torches (twin or tandem), and dynamic control of the wire feeding.

In general, it is assumed that GMAW has a strict co-dependency between deposition rates and arc energy. The one factor limiting the increase in productivity is excessive heat input (directly related to arc energy) and consequently causing metallurgical problems, more thermal stress (distortion/residual stresses), and oxidation. The melting rate of the wire in GMAW is usually correlated to two effects: the energy dissipation in the anodic sheath plus the ohmic heating in the electrified length of the wire (between the contact tip and the beginning of the arc) [1]. From this concept, one way to decrease welding current is to select wires with smaller diameters to increase the ohmic heating and consequently melting rate for a given current level. Similarly, increasing the contact tip to work distance (CTWD) while

---

Recommended for publication by Commission XII - Arc Welding Processes and Production Systems.

✉ Fernando Matos Scotti  
fernando.scotti@linde.com

<sup>1</sup> Linde GmbH, Carl-Von-Linde Straße 25,  
85716 Unterschleißheim, Germany

<sup>2</sup> Production Technology Group, Technische Universität  
Ilmenau, Gustav-Kirchhoff-Platz 2, 98693 Ilmenau, Germany

<sup>3</sup> European School of Materials Science and Engineering,  
Université de Lorraine, 6 Rue Bastien Lepage, BP 630,  
54010 Nancy, France

keeping the same arc length will increase the electrified length and hence also allow a reduction in current. The effect of CTWD variation on GMAW was explored by [2] which showed that around 7 A of current can be reduced per millimeter of stickout increased (for a wire diameter of 1.2 mm). Furthermore, the reduction in current resulted in lower penetration of the weld beads. However, both approaches have narrow working envelopes. Thinner wires are harder to manufacture (increase costs) and require high wire feed rates in high deposition rate applications, which can cause feedability problems. Increasing the CTWD is also limited since the shielding gas coverage can be compromised and further due to the memory shape of the spooled wire (cast and helix) long electrode lengths can cause difficulties in the welding direction in relation to the torch positioning. In a study investigating the potential of reducing energy input in wire arc additive manufacturing by increasing CTWD, the authors mentioned this deviation in the desired wire position as a limiting factor [3].

Depending on parameters such as wire feed speed, voltage, and shielding gas composition, the GMAW can present different metal transfer modes, related to how the metal is transferred from the wire to the molten pool. Scotti and Ponomarev [4] described and classified the metal transfer modes in detail and divided them into classes: natural, controlled, or interchangeable metal transfer. The characteristics of the transfer mode have to be taken into consideration depending on the application, and the correct selection may allow a proper balance between quality and productivity [5]. Short circuiting mode is generally used for root passes or thin plates, operations in which heat input must be limited. In controlled short circuiting, the use of current waveform control allows reduction of spatter and increased stability. Natural spray arc is usually related to high power and is not usually applied for thin plates or for welding out of position. Thus, a controlled spray arc, which can be done through direct or alternating current pulsed waveform is used to achieve free flight transfer with lower average current levels. The results from [6] and [7] show that different transfer modes also have an influence on the thermal efficiency (heat transferred to the plate) where short arc presented higher efficiency, followed by pulsed which is still lower than natural spray arc.

As the controlled waveforms have been thoroughly investigated and improved in the past years, the ability to further affect arc energy and heat input while still being capable of achieving proper metal transfer characteristics would further expand the possibilities within the GMAW process. Actively preheating the wire would have advantages in the same direction of increasing CTWD (decreasing welding current); however, with more flexibility in terms of physical disposition (avoiding problems with gas coverage and wire direction) and in terms of control by allowing variations in

the preheating levels according to needs. Additional wire preheating based on ohmic effect was explored by [8, 9], where the authors showed that an increase in deposition rates could be achieved while maintaining the same dilution level by preheating the wire in GMAW. Alternatively, other authors [10] have used a gas tungsten arc (TIG) established between the non-consumable electrode and the wire prior to the main GMAW arc. Similar results were observed in terms of reduction in arc energy as well as in dilution. Although the results in the literature show potential for active wire preheating, no further developments could be found towards the performance of such torches under realistic conditions and no functioning commercial solution is available in the market.

The torch henceforward presented is a development from Linde GmbH arc technologies laboratory and is entitled Joule Torch, which is based on two different electric circuits: one being connected to a hotwire power supply that preheats the wire by means of Joule effect (between two contact tips within the torch) and a second circuit functioning as in standard GMAW between the second contact tip and the workpiece, through which the arc is established. As an initial exploration of the potential of controlling heat input into the workpiece and/or increasing productivity with such technology, a welding case of mild steel lap joint in horizontal position was selected. Thus, the objective of this work is to evaluate the potential of joule heated (JH)-GMAW in influencing heat input and bead formation in mild steel welding and the feasibility of its combination with pulsed arc mode. Specifically, it aims to verify whether the effects of wire preheating remain practical in a real welding joint where bead alignment has an impact.

## 2 Methodology and experimental procedure

As previously introduced, this work situates within the developing stage of a novel GMAW variant, hereby called JH-GMAW. The torch comprises a preheating circuit established between two contact tips through which the wire runs and is heated by the ohmic effect (Fig. 1) through a constant current power source. The extent of preheating will depend on the current level in the preheating circuit as well as the distance between the contact tips (represented by  $l_{PH}$  in the schematic). Finally, a circuit between the lower contact tip and the base metal (as in standard GMAW) is implemented through which an arc is established. Since in standard GMAW, the effect of joule heating in the electrified length of the wire can be also considered preheating, from hereon, the added preheating by the additional circuit will be referred to as

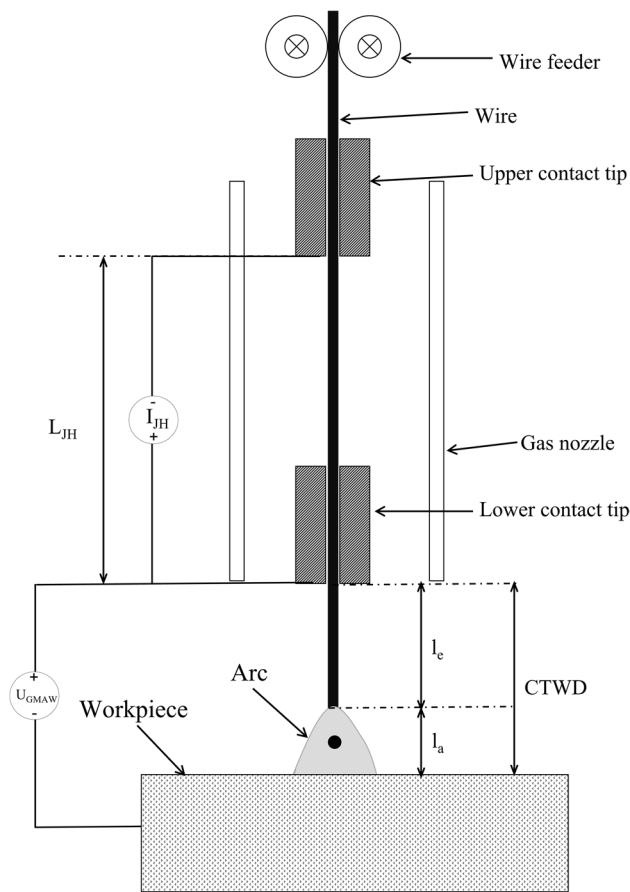


**Fig. 1** Schematics working principle of active joule wire preheating in GMAW

active preheating, whereas the preheating in the GMAW circuit (which also happens in the standard process) will be referred to as passive preheating.

In the first step for this work, a series of bead-on-plate welds were carried out to identify the effect of varying the preheating current for different wire feeding speeds over the electric parameters in the arc circuit. Even though the torch can be used in any of the metal transfer modes applicable for GMAW, the pulsed current (GMAW-P) mode was selected to guarantee a stable and continuous free flight droplet transfer. Based on the results from this first step, a series of conditions were selected to be tested on lap joints welded in horizontal position (PC according to ISO 6947 [11]) in two different combinations of plate thicknesses. Such conditions are aimed at maintaining the deposited bead area and varying preheating levels for different wire feed speed ( $v_w$ ) and travel speed ( $v_T$ ) combinations. During welding, the electric signals (current and voltage for both circuits) were recorded, as well as thermographic images of the plate. The resulting welds were analyzed regarding the bead formation through prepared cross-sections, as well as microhardness tests.

## 2.1 Experimental planning, materials, and procedures

All welding trials were performed on an automated setup based on a numerically controlled (CNC) set of motorized axes with three coordinates. For the GMAW circuit, an EWM Alpha Q 552 power source was used and for the preheating circuit an EWM Tetrix 300. All welds were done with standard G3Si wire with 1.2 mm in diameter, and shielding gas coverage was based on the composition 8.0%  $\text{CO}_2$  + 92.0% argon at a flow rate of 18 L/min. For each circuit, independent measurements of current and voltage were recorded at a rate of 10 kHz throughout the welds. The wire feed speed was verified through an encoder installed on the wire feeder inlet. Additionally, for the lap joint welding, an infrared thermal camera was installed on the backside of the plates (avoiding arc interferences) to record the thermal field in the plate with an adjusted emissivity of 0.8, covering a range from 525–1100 °C. Additionally, a high dynamic range camera for welding processes was used for process monitoring. A schematic of the experimental rig is shown in Fig. 2. Finally, for each weld, three cross-sections were cut, ground, etched, and analyzed through optical microscopy. The fusion zone areas were measured by image correlation in the cross-sections and the reported results consist of the average of three measurements (in different sections) per test coupon. The Vickers microhardness tests were performed using 0.5 kg of load and 0.5-mm spacing between indentations.

In the initial step, a large mild steel plate (300 × 400 × 12 mm) was used to perform multiple blind welds. A copper plate with water cooling was used to guarantee that the base plate reached ambient temperature before starting new welds. In this step for three wire feed speeds (6.5, 8.0, and 9.5 m/min), the standard process (without preheating) was tested, and the preheating currents ( $I_{JH}$ ) were selected starting from 55 to 115 A. For each case, the voltage correction was varied to guarantee a proper arc length for GMAW-P, meaning the arc was not too short that short circuits were frequent and not too long to avoid instabilities.

The selected joint for this study is based on two plates (S355 mild steel) with thicknesses of 4 mm in both plates (referred as 4 and 4 in Table 1), and a second condition where a 4 and 3 mm (as 3 and 4 in Table 1) plates were joined. In both cases, the plates are positioned vertically and formed a lap joint. To maintain the deposited area of the welds different combinations of wire feed speed ( $v_w$ ) and travel speeds ( $v_T$ ) were selected, resulting in the same ratio, as shown in Table 1. The estimated weld bead area (calculated by the ratio between  $v_w$  and  $v_T$  and multiplied by the cross-sectional area of the wire) is shown as  $W_A$ . For the condition where 4 and 3-mm plates were welded, the ratio was slightly varied. For each of these, two preheating levels (low

**Fig. 2** Experimental setup rig schematics for lap joint welding in horizontal position (PC); contact tip to work distance: 17 mm; work angle 50°; travel angle 15°

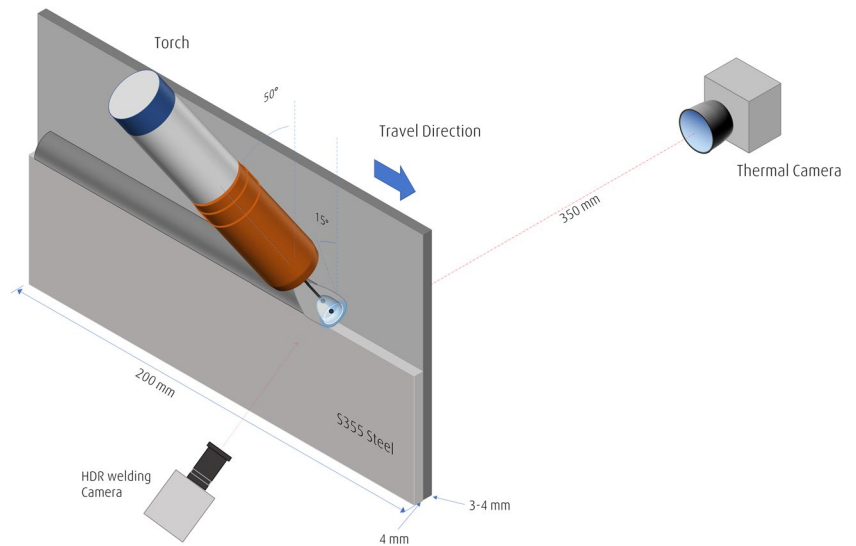


**Table 1** Experimental planning for lap joint welds ( $v_w$ : wire feed speed;  $v_T$ : travel speed;  $I_{JH}$ : wire active preheating current)

Test number	Plate thickness (mm)	$v_w$ (m/min)	$v_T$ (cm/min)	$W_A$ (mm <sup>2</sup> )	$I_{JH}$ (A)
1	4 and 4	6.5	51		0
2				14.4	60
3					90
4	4 and 4	7.5	57		0
5				14.8	65
6					95
7	4 and 3	7.2	60		0
8				13.6	65
9					95

and high) were selected by interpolating the results from the preliminary step as well as a reference with no preheating.

### 3 Results and discussions

#### 3.1 Preliminary results on the effects of active preheating on melting rate

Figure 3(a) shows the graphs for the arc currents reached as a function of the preheating current for different wire feed speeds ( $v_w$ ). The measurements of  $v_w$  confirmed that for a set wire feed speed value in the machine, the average value of the measured  $v_w$  was maintained independent of the preheating. This confirms that the synergic mode of the power

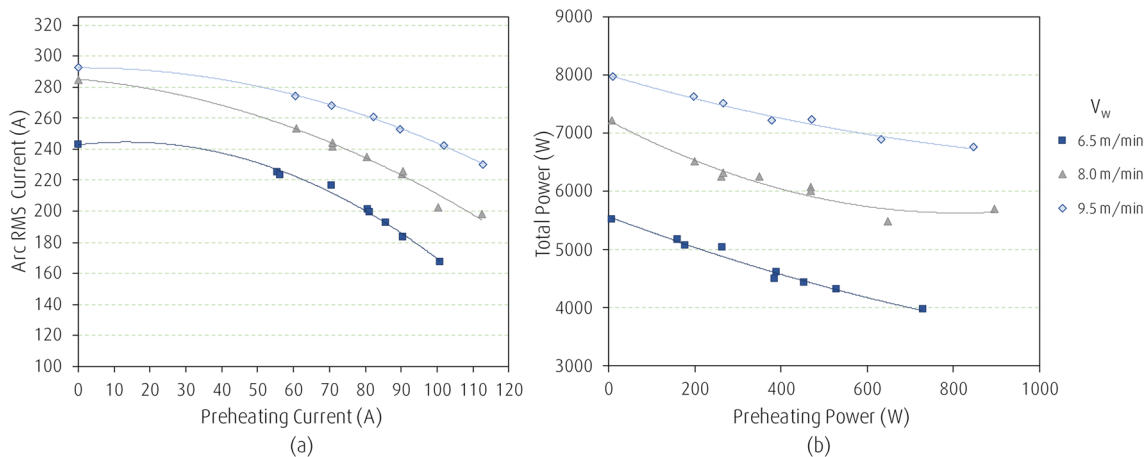


**Fig. 3** **a** Mean arc current as a function of preheating current; **b** total preheating (sum of GMAW circuit and preheating circuit powers) as a function of preheating power for bead on plate welds for three wire feed speeds

supply did not act over the wire feed speed to control the process. As can be seen, the general trend for each  $v_w$  is to reduce the arc current, and the higher becomes the preheating current. Figure 3(b) shows that even though the joule heating adds to the power of the process, the overall power decreases due to the reduction in the GMAW arc current. This means that considering the total power employed for a given wire feed speed, the preheating increases melting efficiency. Although only three different wire feed speeds are shown, the trends allow for interpolation and estimation of the resulting currents for any  $v_w$  values within the tested range.

The results indicate the active preheating of the wire still allows for a stable and continuous melting with a lower GMAW arc current. The melting rate equation used for standard GMAW would have a third term related to the preheating, as shown in Eq. (1) (adapted from [1]). Where  $I_{GMAW}$  corresponds to the main current, the Greek letters  $\alpha$ ,  $\beta$ , and  $\gamma$  correspond to constants depending on the thermophysical properties of the material;  $L_e$  corresponds to the electrified length of the wire in the GMAW circuit; and finally,  $L_{JH}$  and  $I_{JH}$  correspond to the active heating length (in the secondary circuit) and preheating current.

$$MR = \underbrace{\alpha I_{GMAW}}_{\text{Effect of arc attachment}} + \underbrace{\beta \frac{L_e I_{GMAW}^2}{A_w}}_{\text{Passive Jouleheating}} + \underbrace{\gamma \frac{L_{JH} I_{JH}^2}{A_w}}_{\text{Active Jouleheating}} \quad (1)$$

It is reasonable to assume that the passive Joule heating portion of the equation depends on the wire temperature since resistivity will increase. Thus, it can be expected that preheating has a direct effect on reducing GMAW energy, since the wire is already heated, but at the same time boosting the passive preheating happening in the wire due to the GMAW circuit. Furthermore, the wire feed speed itself will influence the available time for the wire to be preheated within the heating circuit.

The synergic mode from the power supply designed for standard GMAW-P for 1.2-mm-mild steel wire was used for all tests without modifications other than the voltage correction. For all cases when the preheating was increased, without modifying the voltage correction, an increase in arc length was observed. This is a consequence of the reduction in the current needed to melt the wire, meaning a higher voltage available will result in higher arc length. Thus, a reduction in voltage is done so that the voltage is compatible with the lower current. As a rule, a similar arc length was adjusted for all cases, by reducing the voltage correction setting, in such a way that the arc was not too low (with the occurrence of short circuits) or not too high (unstable). In some cases, a limit of preheating was reached in which it was no longer possible to adjust the arc length to acceptable levels. However, this can be attributed to a limitation in the synergic algorithm which was not specifically designed for the addition of preheating. Figure 4 shows typical current and voltage diagrams for a time frame period of 0.1 s. One

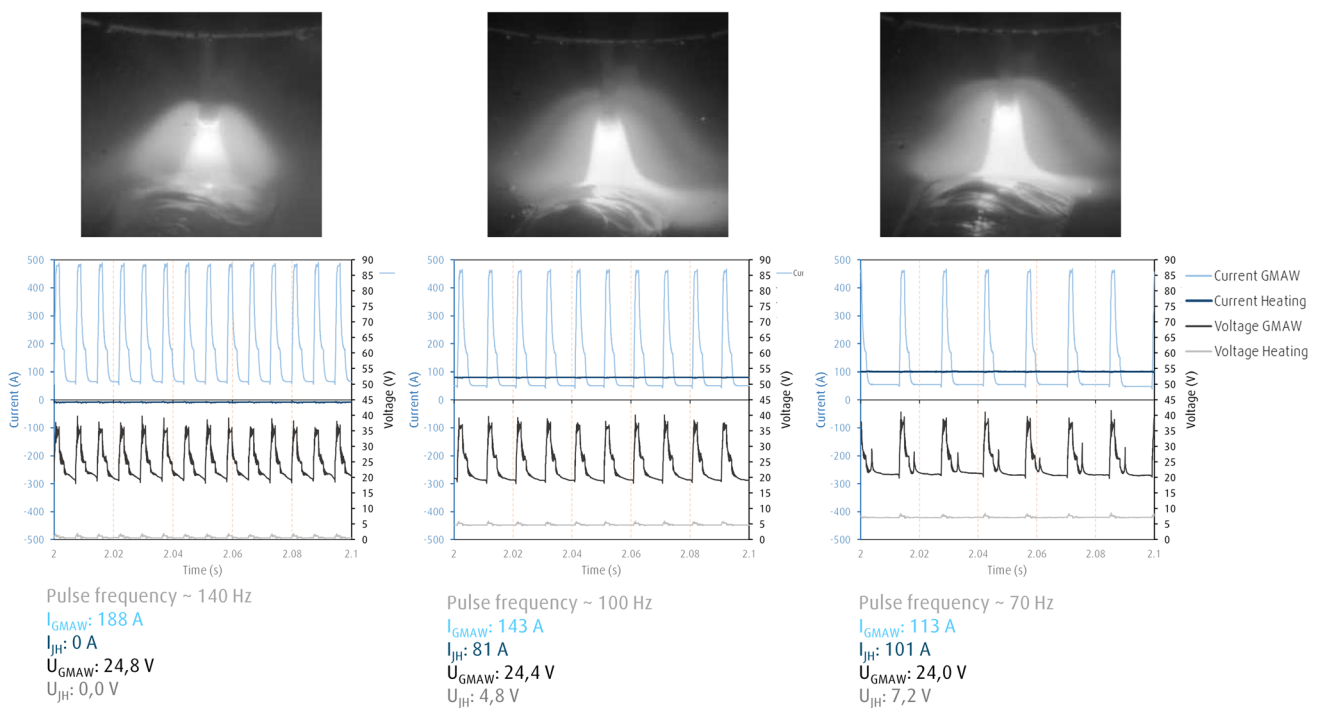


Fig. 4 Current and voltage diagrams for different preheating currents and average of measured values

can notice that for the mode utilized, the main change in current waveform was based on reducing the frequency while keeping the other parameters unchanged. However, other parameters could also be modified as far as finally the power levels are adequate to melt the given  $v_w$  (i.e., the melting rate equation is fulfilled). The reduction in frequency, while keeping a high peak current, could cause the formation of big droplets which would tend to explode into small spatter. Thus, for the subsequent welding tests in the lap joints, a modification in the synergic program was made so that a lower peak current could be used in the cases where preheating was applied.

### 3.2 GMAW current and arc energy per unit length behavior in the lap joint welds

As mentioned in Section 2, for the joint selected in this case study, a fixed approximated weld bead area was kept constant. This means that since the wire was unchanged (1.2 mm in diameter) the ratio between wire feed speed and travel speed was kept constant (same amount of material deposited per unit length). The graphs in Figure 5 present the resulting arc rms current and arc energy per unit length (calculated by the division of the average instantaneous power by the travel speed). Between the two different  $v_w$ , the effect of the corresponding travel speed brought the energy levels to similar values when similar preheating conditions were applied. It is important to mention that no efficiency factor was multiplied (normally used to convert arc energy into heat input). Although the efficiency of GMAW-P has been investigated in the past, it is unclear if the same factor is realistic when active preheating is applied. For this reason, the subsequent analysis will focus on evidence of changes in the thermal behavior in the welded plate as well as in the resultant beads.

In general, following the previously discussed reduction in GMAW power due to increased preheating, this result can be reflected in the arc energy for a given  $v_w$ . From 0 to mid-level preheating (60–65 A), the reduction in arc energy was 15%; further comparing mid-level with high level preheating (90–95 A), the energy decreases by 18%. This effect is attributed to the quadratic relation between current and power in the preheating circuit.

### 3.3 Molten pool and weld bead formation

One of the challenges in welding out of position is to avoid sagging of the molten pool. In the high dynamic range photographs, shown in Fig. 6, the dashed line helps identify the plate edge whereas the molten pool is seen in gray color (case of 4 and 4-mm plates). The higher preheating current and the consequent reduction in arc energy resulted in a narrower and shorter molten pool, especially towards the back in the travel direction. The slags can be seen as oval brighter spots floating in the molten pool and indicate the boundary between liquid and solid metal. In the standard process (without active preheating) a bigger portion of the molten pool hangs to the side and increases the risk of collapse or sagging. For both tested wire feed speeds, the behavior was similar. The resulting cross-sections further confirm the result and a trend of the fused zone being dislocated towards the left side and downwards is seen with higher arc energy. Additionally, the formation of undercut can be seen especially when no preheating was used. With  $I_{JH}$  65 A the undercut is still present but smaller, and finally no undercut is seen for  $I_{JH}$  95 A. A possible explanation is that the lack of material area on the upper toe of the weld allows the arc pressure (which is also higher when no preheating is used — due to the higher current levels) digs into the

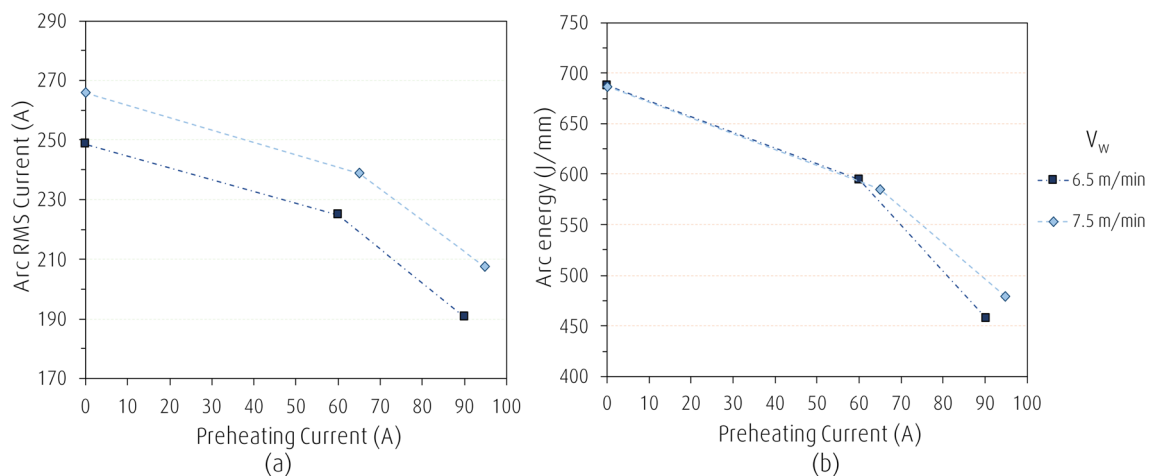


**Fig. 5** RMS current values (a) and arc energy per unit length (b) measured for lap joint welding conditions as a function of active preheating current

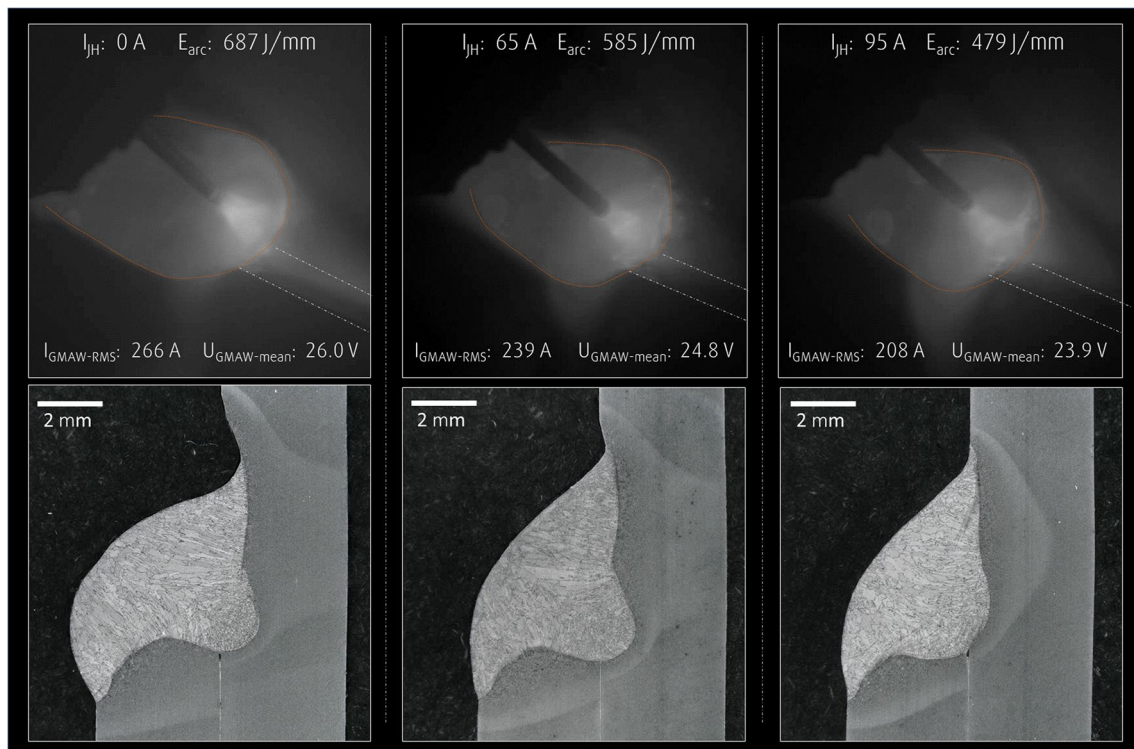


**Fig. 6** Molten pool behavior for different preheating currents and the resulting cross section ( $v_w$ : 7.5 m/min;  $v_T$ : 57 cm/min; 4 and 4-mm plates)

base plate causing undercuts. The fusion zone profile for the case of  $I_{JH}$ : 95 A presents a wider penetration profile or a less pronounced argon finger shape. It can be expected that the reduction of 22% in RMS current from 0 to 95 A in  $I_{JH}$  impacted the arc pressure acting over the molten pool (especially considering the travel speed is the same). Besides that, results from the literature show that droplet size and location of impingement in the molten pool can also affect the bead formation [12, 13]. In this case, the change in pulsing frequency may have affected droplet size and speed, resulting in variation in the bead profile (argon finger shape). In the case of lap joints with a gap between the plates, this bead profile would be favorable to guarantee proper bridging.

It is worth noting that in this type of joint, the torch positioning and the direction of the arc attachment is crucial for guaranteeing a stable molten pool. For this reason, increasing the CTWD would potentially make it difficult for automation and path programming due to deviations in the wire position. The active wire preheating allowed a suitable molten pool to be maintained while keeping the same CTWD. On the tested ranges the preheating of the wire did not cause any geometric deviations on its path, meaning the torch position and path program could be kept the same.

Further evidence of the heat input reduction with higher preheating levels can be seen by the measurements of the fusion zone area in Fig. 7. For this type of joint, the dilution cannot be easily estimated since the original edge of the

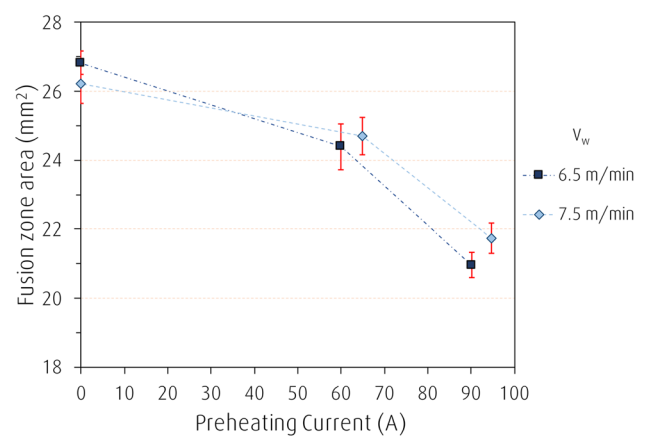


**Fig. 7** Measured values of fusion zone area; red error bars correspond to standard deviation (4 and 4-mm plates)

lower plate is not identifiable in the cross-section. However, since the ratio between  $v_w$  and  $v_T$  was the same, and the deposition efficiency should not vary significantly between the tests (all tests showed a low level of spatter generation), the amount of material deposited per unit length can be assumed to be constant. Thus, the variation in fusion zone area can be attributed directly to a bigger volume of molten base metal in the bead formation. The graph follows a similar trend as the arc energy shown in Fig. 5. This result indeed shows

that the reduction in arc power due to the active preheating impacts the heat input into the workpiece and leads to a lower amount of base metal melting. Considering 7.5 m/min from 0 to 65 A in  $I_{JH}$  reduces by 6% and further from 65 to 95 A, the reduction is 12%. The increased effect for the high preheating level is also compatible if the quadratic influence of preheating current observed in current values and arc energy. When comparing the two different  $v_w$ , the fused areas reach values with no statistically significant differences when the preheating was on a similar level (resulting in close values for arc energy shown in Fig. 5). Except for high preheating (90–95 A) where indeed the lower arc energy achieved with 6.5 m/min resulted in a smaller fusion zone area.

### 3.4 Thermal field in horizontal lap joints

Figure 8 shows single frames of thermal images recorded on the backside of the plates during welding. It can be assumed that while moving the thermal field assumes a quasi-steady state condition. For each  $v_w$  (6.5 and 7.5 m/min), the effects of increasing preheating (and consequently decreasing arc energy — from left to right in the image are clearly seen, not only as a reduction in the area of maximum temperature within a frame but also in the area covered by the isotherms (regions with same temperature/color). The comparison between the tests where the arc energy is close and the  $v_w$  values are different (comparing upper and lower row) except for conditions with  $I_{JH}$ : 0 A even a variation of 14 to 19 J/mm resulted in a thermal field with higher temperatures. For  $I_{JH}$ : 0 A despite the energy being lower, the condition with  $v_w$ : 7.5 m/min resulted in higher temperatures. However, as

shown in the fusion zone area results, the experimental variability within tests with close arc energy resulted in less significant changes than the effect of preheating current. Meaning the results allow to conclude that preheating impacted the heat transference to the plate regardless of the wire feed speed.

It can be expected that the difference in thermal fields between the tested conditions will affect the size and morphologies in the heat-affected zone, which will further be discussed in the following section. Besides the metallurgical characteristics, on the surface aspect of the welds shown in Fig. 9, it can first be noticed that in the top surface, the bead not only becomes more regular with higher preheating but also the amount of slag is reduced. A study has shown that slag formation is a function of oxidizing time and oxidizing potential [14]. The lower arc energy (and voltage) associated with higher preheating may have reduced the oxidizing potential as well as the exposure from the molten metal (in the droplet and molten pool) to oxygen. An additional hypothesis that a lower dilution (less mixing between filler and base metal) could justify a lower amount of slag former elements (Si and Mn) available in the molten pool surface. The results for thermographic images from the backside results shown in Fig. 8 are consistent oxidation aspect. When no preheating was applied, the temperatures and exposure time in the back surface were high enough that a flaking oxidation layer was formed. Oppositely, when preheating was applied only coloration is observed. The case of 7.5 m/min was chosen, but the same behavior in relation to different preheating currents was observed with 6.5 m/min. Beyond the presence of undercuts, this heavy oxidized layer seen in the standard case would require an extra step of cleaning in case the structure has to be painted. Assuming stainless steel

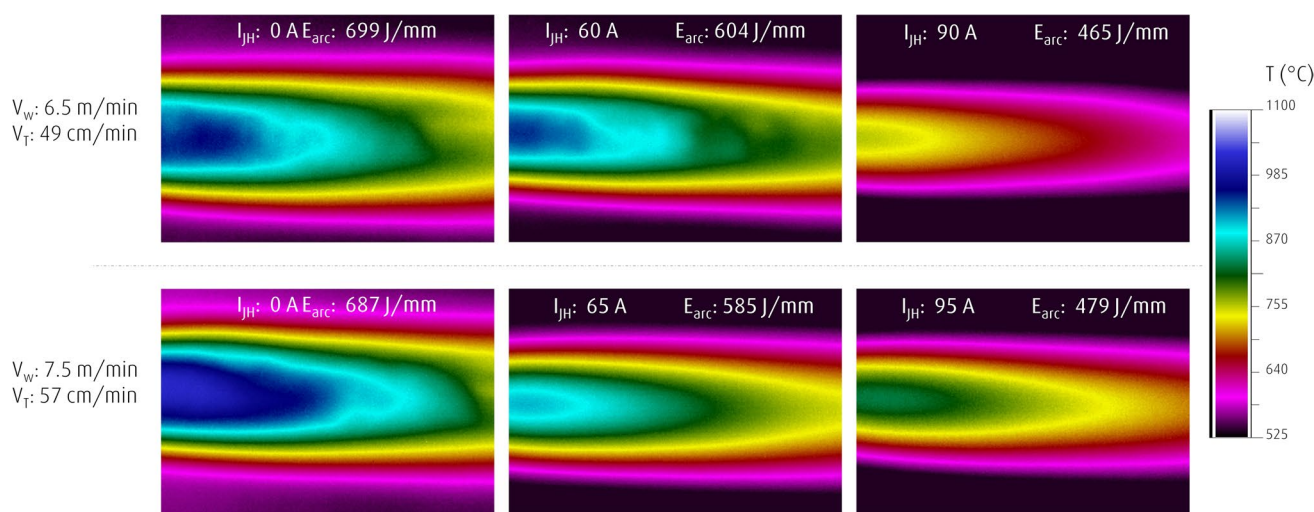


**Fig. 8** Thermographic images taken from the backside of the welds for different  $v_w$  and  $I_{JH}$  conditions and resulting arc energy ( $E_{arc}$  — average instantaneous power divided by travel speed)



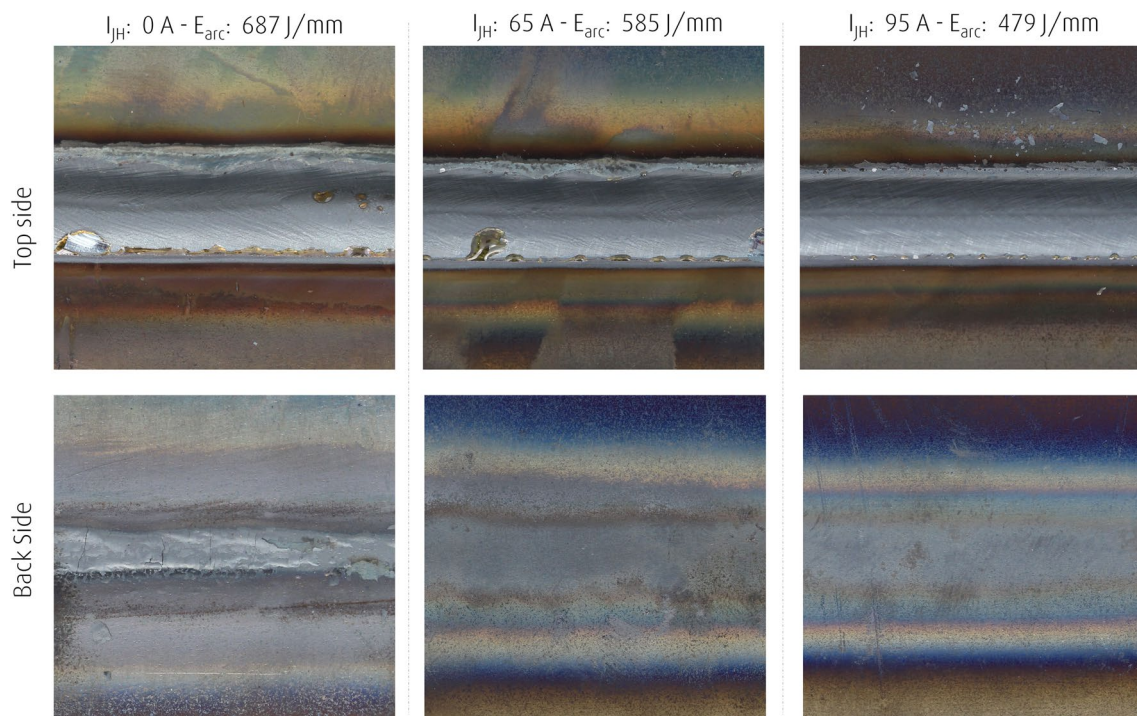


**Fig. 9** Photographs of top and back side of welded plates with different active preheating conditions ( $v_w$ : 7.5 m/min;  $v_T$ : 57 cm/min)

would follow the same trends, the oxidation would impact the corrosion resistance negatively.

### 3.5 Heat-affected zone microstructure and microhardness

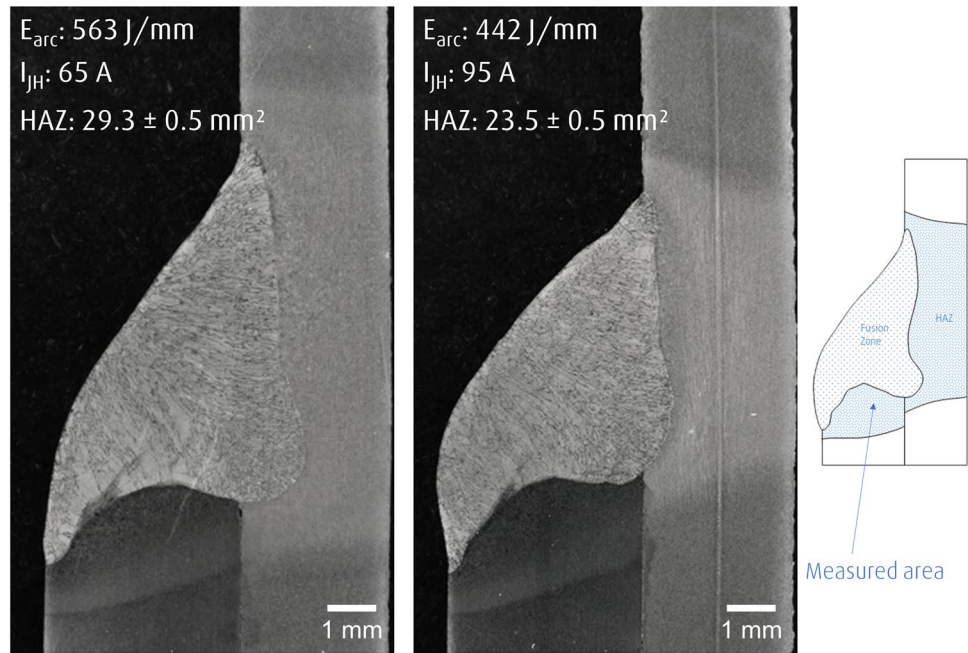
The analysis of the effects in the heat-affected zones was based on the case of 4 and 3-mm plates with medium and high preheating (65 and 95 A), since for these conditions the weld beads showed no undercut and the oxidation in the backside stayed within acceptable levels. Additionally, the thinner plate had a bigger sensitivity to heat input. However, the same behavior and effects discussed ahead are valid for 4-mm thickness. Initially, the heat-affected zones were analyzed in general without discerning their subzones and the area was measured considering the brighter regions revealed by the etching in the vicinity of the fusion zone. The results are presented in Fig. 10. Along with the reduction in fusion zone area discussed previously, the lower arc energy resulted in a significantly smaller heat affected zone (18% lower in area). The impact is especially noticeable in the 3-mm plate. As far as the weld bead dimensions are in accordance with requirements, a smaller HAZ is usually preferable as it corresponds to less alteration in the base metal microstructure, resulting in less potential harm to mechanical properties.

Figure 11 shows micrographs of the heat-affected zones near the deepest penetration areas (in the same orientation as the macrographs in Fig. 10). The coarse grain heat-affected

zone (CGHAZ) corresponds to the regions where the temperature was well above the upper critical temperature  $A_{c3}$  (usually between 723 and 900 °C for low alloy steels [15]) where a fully austenitic microstructure is formed [16]. The longer time within this range allows more severe grain growth. During cooling, the austenite decomposes into grain boundary ferrite, Widmanstätten ferrite, and pearlite. The white bands in the microstructures shown in Fig. 11 correspond to the ferrite and specifically those forming polygonal shapes are grain boundary ferrite, which are formed on the previous austenitic grain boundaries. The size of these polygons indicates the magnitude of grain growth in the CGHAZ. When comparing the two cases, it is noticeable that with higher arc energy (i.e., lower wire preheating) the grains grow larger, and the extension of the grain growth area is larger (in this case extending all along the visible frame). Whereas with low energy, the grains are finer and after around 0.4 mm, the fine grain heat-affected zone (FGHAZ) is reached.

Although in the present study, a low carbon and low alloy steel was used, trends presented can be potentially applied for alloys that are more sensitive to phase transformations, allowing further benefits. As the grain size will influence the quenching ability, a coarser CGHAZ would be critical in the case of alloys with susceptibility to the formation of hard phases such as martensite. Furthermore, researchers have correlated the impact of coarser grains in the CGHAZ with a reduction in toughness for different alloys [17, 18].

**Fig. 10** Cross sections and heat-affected zone (HAZ) areas for  $I_{JH}$ : 65 and 95 A ( $v_w$ : 7.2 m/min;  $v_f$ : 60 cm/min; 4 and 3-mm plates) — blue area in the sketch exemplifies how the HAZ area was measured (base material: S355 mild steel)



In Fig. 12, the results for microhardness lines made 1 mm apart from the lower edge of the 3-mm plates show that the aforementioned impacts in the HAZ have also an impact on hardness values. The extension in which the microhardness values deviate from the base metal (168 HV) is smaller

when a preheating value of 95 A was used. Furthermore, the maximum hardness reached was significantly lower. In the exemplified microstructure images above the graph, in this position (at the same distance from the plate edges) the microstructure is more refined with lower energy, and the vertical lines indicate that the preferential direction originated from the hot rolling process when the plate was manufactured is still visible. Whereas when the energy was higher (lower preheating), partial transformation occurred, and the ferrite presents a coarser morphology.

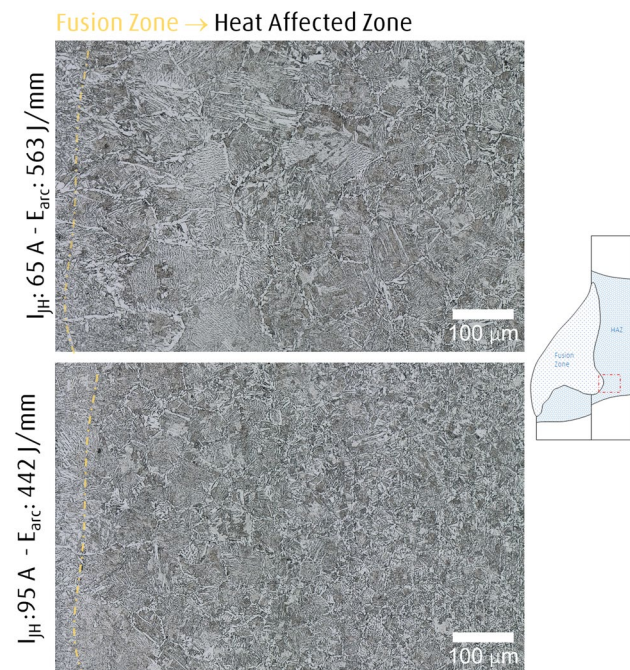


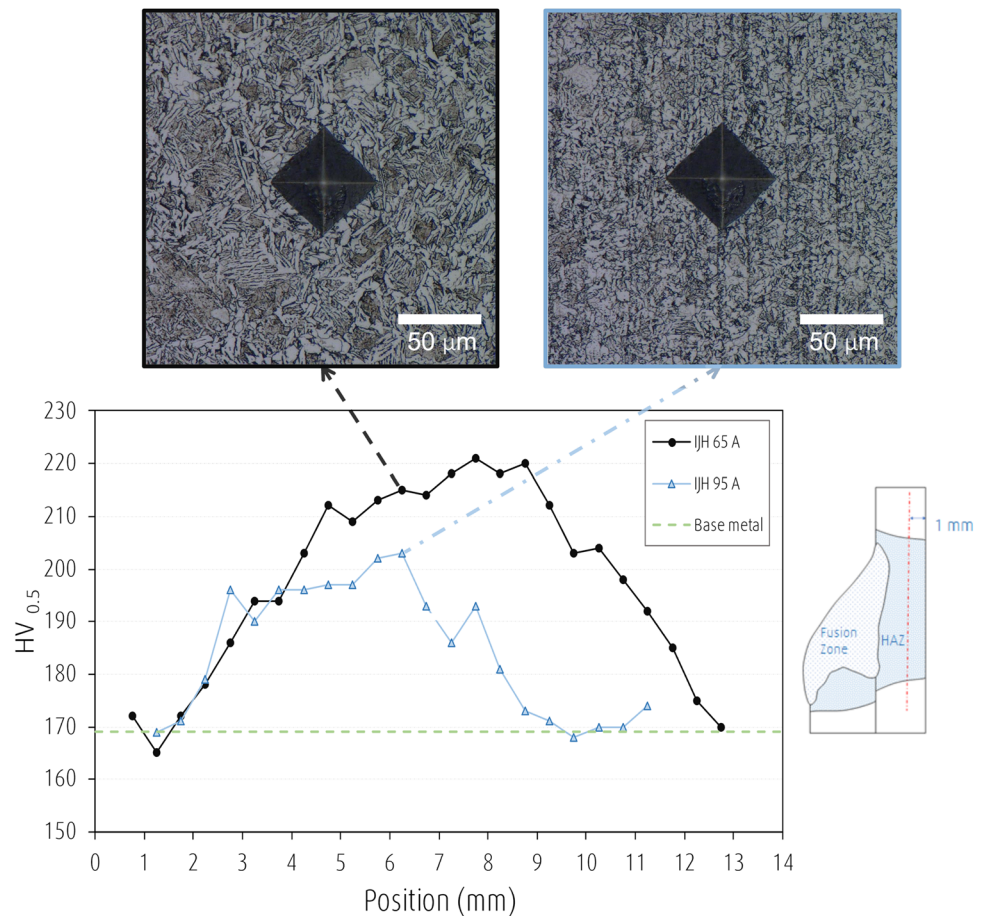
**Fig. 11** Micrographs in the heat affect zones for  $I_{JH}$ : 65 and 95 A ( $v_w$ : 7.2 m/min;  $v_f$ : 60 cm/min; 4 and 3-mm plates; base material: S355 mild steel)

### 4 Conclusions

In the current study, a concept for heat input control through active wire preheating utilizing joule heating was presented, and its performance was tested on the execution of lap joint welds in horizontal position. The results showed that for a given wire feed speed, increasing the preheating current allowed a significant reduction in the current levels necessary to maintain the wire melting. The effect of wire preheating could be easily adapted to a standard pulsed mode GMAW by properly reducing the voltage so that a proper arc length was formed.

The reduction in arc power (and consequently in arc energy) allowed by the preheating improved the ability to maintain a stable molten pool when welding in horizontal position. With high arc energy, the molten pool becomes bigger and tends to sag down, also increasing the risk of undercut formation. The wire preheating had no negative effect in the wire positioning, and the weld beads were

**Fig. 12** Vickers microhardness results for  $I_{JH}$ : 65 and 95 A ( $v_w$ : 7.2 m/min;  $v_T$ : 60 cm/min; 4 and 3-mm plates; base material: (S355 mild steel))



properly directed. Multiple methods were used to verify the correlation between arc energy and heat input and its effects in the resulting weld. Through thermographic images, it was shown that increasing preheating currents resulted in lower maximum temperature and smaller thermal fields in the backside of the plate. This result was reinforced by analyzing the oxidation level in the plate surface, where when no preheating is used a flaking layer of oxide is formed, whereas with preheating only an effect of coloration was seen.

Finally, through the microstructure analysis, the results showed that the impact of varying preheating current significantly affects not only the heat affected zone size (which becomes smaller as the arc energy is reduced) but also the morphology of the HAZ subzones. This ability to impact the microstructure formation while maintaining the same deposition rate can further be used to improve or make it possible to weld materials with lower weldability.

**Acknowledgements** The authors thank Linde's Arc Technologies working team and Linde Technology management for the direct and indirect support through the conduction of this research.

## Declarations

**Conflict of interest** The authors declare no competing interests.

## References

1. Palani PK, Murugan N (2006) Selection of parameters of pulsed current gas metal arc welding. *J Mater Process Technol* 172:1–10. <https://doi.org/10.1016/j.jmatprotec.2005.07.013>
2. e Silva RHG, dos Santos Paes LE, Barbosa RC et al (2018) Assessing the effects of solid wire electrode extension (stick out) increase in MIG/MAG welding. *J Braz Soc Mech Sci Eng* 40:31. <https://doi.org/10.1007/s40430-017-0948-9>
3. Henckell P, Gierth M, Ali Y et al (2020) Reduction of energy input in wire arc additive manufacturing (WAAM) with gas metal arc welding (GMAW). *Materials* 13:2491. <https://doi.org/10.3390/ma13112491>
4. Scotti A, Ponomarev V, Lucas W (2012) A scientific application oriented classification for metal transfer modes in GMA welding. *J Mater Process Technol* 212:1406–1413. <https://doi.org/10.1016/j.jmatprotec.2012.01.021>
5. Kah P, Latifi H, Suoranta R et al (2014) Usability of arc types in industrial welding. *Int J Mech Mater Eng* 9:15. <https://doi.org/10.1186/s40712-014-0015-6>
6. Haelsig A, Kusch M, Mayr P (2015) Calorimetric analyses of the comprehensive heat flow for gas metal arc welding. *Weld World* 59:191–199. <https://doi.org/10.1007/s40194-014-0193-0>
7. Egerland S, Colegrove P (2011) Using solid state calorimetry for measuring gas metal arc welding efficiency. In: Sudnik W (ed) *Arc welding*. InTech
8. Shahi AS, Pandey S (2008) Effect of auxiliary preheating of the filler wire on quality of gas metal arc stainless steel claddings.

- J Mater Eng Perform 17:30–36. <https://doi.org/10.1007/s11665-007-9132-1>
9. Shahi AS, Pandey S, Gill JS (2007) Effect of auxiliary preheating of filler wire on dilution in gas metal arc stainless steel surfacing using RSM. Surf Eng 23:384–390. <https://doi.org/10.1179/174329407X247127>
  10. Ni J, Hongming G (2013) Effect of the wire temperature on the weld formation in GMAW. Adv Mater Res 652–654:1178\*11813. <https://doi.org/10.4028/www.scientific.net/AMR.652-654.2289>
  11. International Organization for Standardization. (2019). Welding and allied processes - Welding positions (ISO 6947:2019). <https://www.iso.org/obp/ui/#iso:std:iso:6947:ed-4:v1:en>
  12. Jorge VL, Scotti FM, Reis RP et al (2020) The potential of wire feed pulsation to influence factors that govern weld penetration in GMA welding. Int J Adv Manuf Technol 110:2685–2701. <https://doi.org/10.1007/s00170-020-06037-8>
  13. Hertel M (2014) Steigerung der Wirtschaftlichkeit der MSGSchweißprozesse durch konsequente Nutzung der Potentiale von Schutzgasen (MSG-Schutzgase). Technische Universität Dresden, Dresden. [https://tu-dresden.de/ing/maschinenwesen/if/fue/forschung/lichtbogenprozesse/projekte/AiF\\_17.431\\_\\_Webpage\\_MSG\\_Schutzgase](https://tu-dresden.de/ing/maschinenwesen/if/fue/forschung/lichtbogenprozesse/projekte/AiF_17.431__Webpage_MSG_Schutzgase)
  14. Derrien R (2011) Understanding the mechanisms underlying the formation of silicate islands in gas metal arc welding. Colorado School of Mines. <https://repository.mines.edu/handle/11124/170385>
  15. Kim H, Inoue J, Okada M, Nagata K (2017) Prediction of  $A_{c3}$  and martensite start temperatures by a data-driven model selection approach. ISIJ Int 57:2229–2236. <https://doi.org/10.2355/isijinternational.ISIJINT-2017-212>
  16. Kou S (2003) Welding metallurgy, 2nd edn. John Wiley & Sons Inc, Hoboken, New Jersey
  17. Wang L, Wu L, He S et al (2023) Effect of heat input on microstructure and impact toughness in the simulated coarse-grained heat-affected zones of X90 pipeline steel. J of Mater Eng and Perform 32:348–365. <https://doi.org/10.1007/s11665-022-07093-9>
  18. Shi M, Di M, Zhang J et al (2021) Effect of initial microstructure on the toughness of coarse-grained heat-affected zone in a microalloyed steel. Materials 14:4760. <https://doi.org/10.3390/ma14164760>

**Publisher's Note** Springer Nature remains neutral with regard to jurisdictional claims in published maps and institutional affiliations.

Springer Nature or its licensor (e.g. a society or other partner) holds exclusive rights to this article under a publishing agreement with the author(s) or other rightsholder(s); author self-archiving of the accepted manuscript version of this article is solely governed by the terms of such publishing agreement and applicable law.